# Biaryl amino acid templates in place of D-Pro-L-Pro in cyclic ß-hairpin cationic antimicrobial peptidomimetics

**Nityakalyani Srinivas,[a] Kerstin Moehle,[a] Khaled Abou-Hadeed,[a] Daniel Obrecht[b] and John A. Robinson*[a]**

***Received 27th April 2007, Accepted 11th July 2007***
***First published as an Advance Article on the web 17th August 2007***
**DOI: 10.1039/b706370a**



The turn-forming D-Pro-L-Pro template has been frequently used to promote regular ß-hairpin conformations in cyclic protein epitope mimetics. Here the use of three isomeric biaryl templates has been studied as alternatives to D-Pro-L-Pro in the preparation of ß-hairpin peptidomimetics. The *o,o′*- *o,m′*- and *m,m′*-isomers of carboxymethyl- and aminomethyl-substituted biaryl templates have been incorporated into novel macrocyclic mimics of the naturally occurring cationic antimicrobial peptide protegrin I. The presence of the *o*-carboxymethyl-*o′*-aminomethyl-biaryl template within the macrocyclic peptide resulted in the appearance of slowly interconverting atropisomers. Although none of the resulting mimetics adopted stable ß-hairpin structures in aqueous solution, they all nevertheless retained a significant antimicrobial activity against Gram positive and Gram negative bacteria. These mimetics provide interesting starting points for an optimization program in the search for potent and novel antimicrobial compounds.

## Introduction

The large class of naturally occurring cationic antimicrobial peptides has attracted great interest recently in the search for new antibiotics to combat the growing threat posed by multiple antibiotic resistant bacteria.[1–4] The antimicrobial peptides discovered so far display divergent sequences and secondary structures, although for many, an underlying common feature is their ability to adopt amphiphilic conformations, with hydrophobic and cationic residues clustered in spatially distinct regions. This can endow on the peptide an ability to selectively bind and disrupt bacterial cell membranes.[3]

Protegrin-I (PG-I), for example, is an 18 amino acid disulfide bridged cationic antimicrobial peptide from porcine leucocytes (Fig. 1),[5,6] which adopts an amphiphilic ß-hairpin structure both in solution and bound to lipid micelles.[7–10] The ß-hairpin structure of PG-I is important for its ability to interact with lipid membranes and its broad spectrum antimicrobial activity.[11–15] Unfortunately, PG-I is also highly hemolytic towards mammalian cells, reflecting a poor selectivity in binding bacterial cell membranes rather than eukaryotic cell membranes. The mechanism(s) underlying this selectivity in membrane binding is (are) still incompletely understood. Macrocyclization is an effective strategy for restricting peptide conformation, and the introduction of semi-rigid linkers or templates provides a further opportunity for influencing the conformation, as well as the biological activity and selectivity.

In previous work,[16–18] we described PG-I peptidomimetics comprising a backbone cyclic peptide attached to a ß-hairpin-inducing D-Pro-L-Pro template (Fig. 1).[19–21] The mimetic **1**, for example, retains much of the antimicrobial activity of PG-I, but shows a much reduced hemolytic activity against human red blood cells, reflecting an enhanced selectivity for bacterial membranes.[17] In this work, we set out to test whether templates based on biaryl amino acids could be used in place of D-Pro-L-Pro to generate new PG-I mimetics with antimicrobial activity.

[a]*Department of Chemistry, University of Zurich, Winterthurerstrasse 190, 8057 Zurich, Switzerland. E-mail: robinson@oci.uzh.ch; Fax: (+41) 1-635-6833*
[b]*Polyphor AG, Gewerbestrasse 14, 4123 Allschwil, Switzerland*

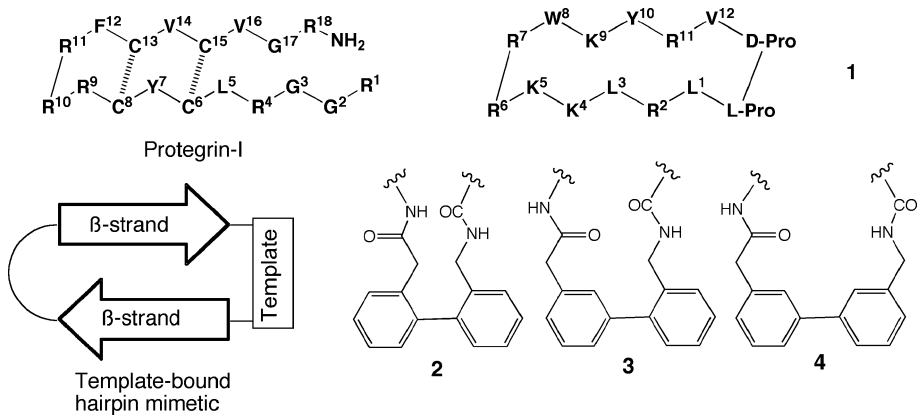


**Fig. 1** Protegrin-I sequence (dashed lines indicate disulfide bridges), template-bound mimetic **1** and the biaryl templates (**2–4**) studied here.

 

Biaryl units represent interesting semi-rigid templates to control peptide conformation. Biaryls occur in many peptide natural products, such as the glycopeptide antibiotic vancomycin, the proteosome inhibitor TMC-95A,[22] and the peptide antibiotic WS-43708A.[23] Biaryl units have also been incorporated previously into various cyclic loop mimetics.[24–28] The biaryl units chosen for study here are the positional isomers **2–4**, which have been inserted directly into the mimetic **1** in place of the D-Pro-L-Pro template.

## Results and discussion

The *o*,*o*′-biphenyl template **2** has been prepared previously from commercially available diphenic anhydride by Brandmeier and Feigel,[24] whereas a related (but not identical) *o*,*m*′-biphenyl template has been prepared by Suich *et al.* using a Suzuki coupling.[25] Here the required Fmoc-protected building blocks **15–17** could all be prepared by the route shown in Scheme 1, which is based on the Suzuki chemistry reported by Suich *et al.*[25] The target peptidomimetics **18–20** were then synthesized by a two-step strategy, using Fmoc solid-phase peptide chemistry to assemble a linear precursor on the resin, followed by a solution-phase macrocyclization and then deprotection (Scheme 2). These mimetics contain the same hairpin sequence as in the mimetic **1**. The desired products were obtained in 50–80% yield after HPLC purification, and each was fully characterized by NMR and MS.

The mimetics **19** and **20** produced in this way showed single peaks upon reverse phase HPLC analysis, and $^1$H NMR spectra were consistent with the presence of one major average conformer in solution. The mimetic **18**, however, behaved differently, showing two peaks in a 1 : 1 ratio by HPLC, which could be separated, but upon re-analysis by HPLC each appeared again as the same two peaks in a 1 : 1 ratio. This is due to the presence of two atropisomeric forms, which interconvert slowly on the HPLC timescale at room temperature. Heating the HPLC column to 60 °C caused the two peaks to coalesce to a single peak. Furthermore, when each step of the assembly of the linear peptide precursor of **18** was followed by HPLC analysis of peptides released from the resin with 95% TFA, all the linear peptides obtained up to and including the coupling of the template showed only a single HPLC peak, whereas linear peptides obtained after coupling valine to the template each appeared as two peaks by HPLC, again consistent with the slow interconversion of diastereomers due to atropisomerism at the biphenyl template within the peptide chain. Variable temperature $^1$H NMR spectra of **18** in aqueous solution also revealed a coalescence of signals over the range 300–330 K, consistent with a faster interconversion of the biaryl atropisomers on the NMR timescale at the elevated temperature.

We also tested whether the rate of atropisomer interconversion around the biaryl link could be slowed down by incorporating the *o*,*o*′-biphenyl template into the smaller macrocyclic peptidomimetic **21** (Scheme 2). This cyclic molecule was prepared in an analogous way, and again appeared upon analysis by HPLC as two peaks. Now, however, the two components could be separated by HPLC and were stable (*i.e.* did not interconvert rapidly) at room temperature. NMR studies in aqueous solution ($H_2O$–$D_2O$ 9 : 1, pH 3, 300 K) were then pursued with these two cyclic mimetics **21a** (elutes first from a C18 reverse phase HPLC column with a MeCN–$H_2O$ gradient of 5–100% MeCN over 30 min) and **21b** (elutes second). Both samples gave $^1$H NMR spectra consistent with a single average conformer present in solution, with all amide bonds *trans*. However, they differed clearly in the pattern of NOE

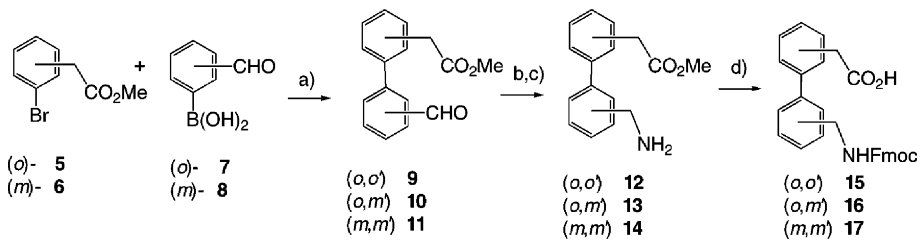


**Scheme 1** Synthetic route to template building blocks **15–17**. *Reagents:* (a) $Pd_2(dba)_3$, P(*o*-Tol)$_3$, 2 M $Na_2CO_3$, MeOH–toluene (1 : 4), 70–80 °C, 16 h; **9** (30%), **10** (85%), **11** (87%). (b) $NH_2OH$·HCl, NaOMe, MeOH 50 °C, 16 h. (c) Pd/C (10%), $H_2$ (1 bar), MeOH, rt, 16 h; **12** (72%), **13** (72%), **14** (85%). (d) i. NaOH, MeOH; ii. FmocOSu, dioxane–$H_2O$, rt, 15 h; **15** (56%), **16** (70%), **17** (70%).

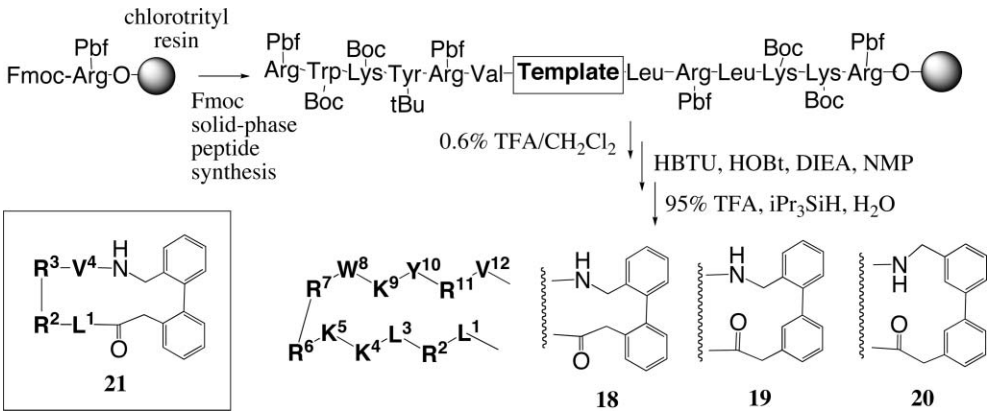


**Scheme 2** Synthesis of the template-bound protegrin mimetics **18–20**, and the small loop mimetic **21**.

contacts observed in 2D NOESY plots. For both, most observed NOEs were intra-residue or sequential, with very few being longer-range NOEs. The resulting NOE-derived distance restraints were used to calculate compatible average solution structures, using the program DYANA.[29] For each molecule, the resulting 20 lowest energy structures are shown in Fig. 2, and statistics from the calculations are given in Table 1.

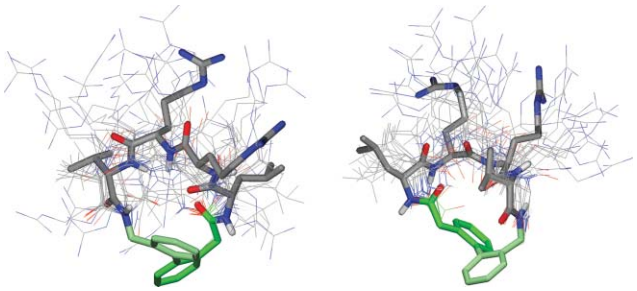

**Fig. 2** Superposition of the final 20 NMR structures for **21a** (left) and **21b** (right), with the N-terminal phenyl ring of the biaryl template pale green and the C-terminal phenyl ring dark green. A single representative NMR structure is represented as a stick model (N atoms blue and O atoms red).

It is notable that for each molecule, the 20 lowest energy backbone conformers populate divergent regions of ϕ/ψ-space (Table 2), although there were no significant NOE violations (Table 1). No regular ß-turn-like conformers are seen within the tetrapeptide motif LRRV. Rather, several residues exhibit ϕ/ψ values in non-allowed regions of Ramachandran space, suggesting either that the structures are strained, or that they represent averages of two or more rapidly interconverting backbone conformations. However, the structure calculations generated unique configurations around the biaryl template, with **21a** having the *S* and **21b** the *R* absolute configuration at the biaryl axis of chirality (Fig. 2). That the biaryl template of type **2** does not stabilize a regular ß-turn or ß-hairpin in the tetrapeptide motif within **21** is consistent with an earlier modelling study, which suggested that the geometry of this *o,o′*-biphenyl template (in at least one configuration) is incompatible with such a ß-turn loop structure,[30] at least when occupying a non-hydrogen-bonding position within a ß-hairpin loop.

**Table 1** Summary of the upper distance restraints and statistics for the NMR structure calculations

| | **21a** | **21b** |
|---|---|---|
| NOE upper-distance limits | 32 | 41 |
| Intraresidue | 12 | 22 |
| Sequential | 20 | 17 |
| Medium- and longe-range | 0 | 2 |
| Residual target function value/Å$^2$ | 0.31 ± 0.01 | 0.42 ± 0.04 |
| Mean rmsd values/Å | | |
| All backbone atoms | 1.17 ± 0.50 | 0.72 ± 0.23 |
| All heavy atoms | 3.31 ± 1.13 | 2.39 ± 0.67 |
| Residual NOE violation | | |
| Number > 0.2 Å | 0 | 2 |
| Maximum/Å | 0 | 0.22 |
| Residues in | | |
| - most favoured ϕ/ψ regions | 1% | 10% |
| - additional allowed ϕ/ψ regions | 55% | 55% |
| - generously allowed ϕ/ψ regions | 28% | 30% |
| - disallowed regions | 16% | 5% |

**Table 2** Averaged backbone torsion angles of the 20 NMR structures

| | | **21a** | **21b** |
|---|---|---|---|
| Leu[1] | Φ | 69.1 ± 95.1 | 43.6 ± 87.0 |
| | ψ | 83.7 ± 52.9 | 134.9 ± 46.4 |
| Arg[2] | Φ | 25.3 ± 94.2 | 35.1 ± 49.4 |
| | ψ | 58.7 ± 29.6 | 68.1 ± 74.8 |
| Arg[3] | Φ | 156.5 ± 70.6 | 62.2 ± 80.2 |
| | ψ | −64.4 ± 18.5 | 169.0 ± 75.0 |
| Val[4] | Φ | −133.3 ± 28.1 | 76.8 ± 94.2 |
| | ψ | 58.5 ± 18.4 | 18.5 ± 2.5 |
| Biaryl[5] | ξ[a] | 130.7 ± 3.2 | −119.8 ± 5.9 |

[a] The torsion is defined as C2–C1–C1′–C2′ from the $NH_2$ to COOH terminus.

Further insights into the solution conformations of **21a** and **21b** were obtained from CD spectra. In the aromatic region (238 nm), **21a** displayed a positive CD peak ([θ] = +3000 deg cm$^2$ dmol$^{-1}$), whereas at this wavelength **21b** showed a very weak negative CD peak ([θ] = −400 deg cm$^2$ dmol$^{-1}$). Earlier studies of the aromatic adsorption bands in the CD spectra of optically active biphenyls have shown that the sign and shape of the curves is dependent upon the type of substituent in the biphenyl nucleus as well as on the absolute configuration.[31–33] For this reason, an unambiguous correlation between the sign of the 238 nm band and the sense of chirality in the template has not been attempted here. On the other hand, in the amide region, larger mirror image-related CD peaks are observed. Thus, **21a** displayed a negative peak at 190 nm ([θ] = −31·500 deg cm$^2$ dmol$^{-1}$) and a positive peak at 212 nm ([θ] = +8400 deg cm$^2$ dmol$^{-1}$), whereas **21b** displayed a positive peak at 190 nm ([θ] = +32·100 deg cm$^2$ dmol$^{-1}$) and a negative one at 212 nm ([θ] = −16·500 deg cm$^2$ dmol$^{-1}$). The shape of the CD curve for **21b** thus resembles those typically seen for ß-sheet structures, whereas that of **21a** resembles more the CD profile of polyproline-II and unordered peptide conformations.[34] These data confirm the divergent chiroptical properties of **21a** and **21b**, and support the proposal that they are related as atropisomers in the biphenyl template.

$^1$H NMR studies were also undertaken on the mimetics **18**, **19**, and **20**. The appearance of two signal sets, for the two interconverting biaryl rotamers of **18**, made complete chemical shift assignments impossible. However, no evidence could be found in 2D NOESY plots of long range NOEs. This suggested that a single stable folded structure is not populated under the conditions used ($H_2O$–$D_2O$, 9 : 1, pH 6). In the case of **19** and **20**, only a single set of signals was observed for each. Again, no long range NOEs were observed, suggesting strongly that a stable fold, such as a ß-hairpin, is not significantly populated in solution. These studies strongly suggest that **18**, **19**, and **20** have relatively flexible (*i.e.* disordered) backbones in aqueous solution. Similar results were found for the peptidomimetic **1** in earlier work.[17]

Finally, the antimicrobial activities of the peptidomimetics **18**, **19**, and **20** were determined by the NCCLS broth microdilution method,[35] using representative gram positive and gram negative test microorganisms. The hemolytic activity was also measured on fresh human red blood cells, as described earlier.[16,17] The results, given in Table 3, show that all three peptidomimetics retain significant antimicrobial activity against all the organisms tested. Moreover, the hemolytic activities of all three are much lower than

 

**Table 3** Antimicrobial activities (minimal inhibitory concentrations (MIC) in μg ml$^{-1}$) and hemolytic activity (% hemolysis of human red blood cells at 100 μg ml$^{-1}$)

| Peptide | *E. coli* (ATCC 25922) | *P. aeruginosa* (ATCC 27853) | *S. aureus* (ATCC 29213) | *S. aureus* (ATCC 25923) | Hemolysis (%) |
|---|---|---|---|---|---|
| **1** | 12 | 6 | 12 | 25 | 1.0 |
| **18** | 64 | 32 | 16 | 16 | 2.5 |
| **19** | 32 | 16 | 8 | 16 | 0 |
| **20** | 16 | 32 | 16 | 16 | 0.2 |

seen with PG-I. Indeed the *o,m′*-biaryl templated mimetic **19** was essentially non-hemolytic under the conditions tested, despite the fact that the biaryl unit is quite hydrophobic in character and might be expected to enhance association of the molecule with a lipid bilayer. The retention of significant antimicrobial activity with all three mimetics is interesting, given that the three templates used have different geometries and will influence the preferred peptide backbone conformation in different ways. Nevertheless, all three mimetics may still be capable of adopting amphiphilic structures in a membrane environment.

One of the most important conclusions of this work is that novel macrocyclic mimetics of PG-I containing the biaryl templates **2–4** can be made, which retain significant antimicrobial activity and show low to zero hemolytic activity. As such, the mimetics **18–20** represent interesting starting points for the discovery of new antimicrobial compounds, whose properties might be further optimized through cycles of combinatorial library synthesis and screening.[16]

## Experimental

### 2-Methyl carboxymethyl-2′-formyl-biphenyl (9)

To a solution of methyl 2-bromophenylacetate (**5**) (4.8 g, 20 mmol) in toluene (100 mL) with aqueous $Na_2CO_3$ (20 mL, 2 M) was added $Pd_2(dba)_3$ (0.6 g, 3 mol%) and P(*o*-tolyl)$_3$ (0.4 g, 6 mol%) followed by 2-formylbenzeneboronic acid (**7**) (2.7 g, 18.2 mmol) in MeOH (25 mL), and the reaction mixture was heated to 70–80 °C under Ar for 16 h, then cooled to 25 °C, diluted with EtOAc, and washed sequentially with aq. $NaHCO_3$, 10% citric acid and brine. The organic layer was dried ($Na_2SO_4$) and concentrated. Flash chromatography (silica, cyclohexane–EtOAc 9 : 1) afforded the desired product **9** as a yellow oil (1.6 g, 30%). $R_f$ (silica, cyclohexane–EtOAc: 3 : 1): 0.4. IR ($CHCl_3$): 1735 s, 1693 s. $^1$H-NMR (300 MHz, $CDCl_3$): 9.65 (s, CHO), 7.98–7.15 (m, 8 arom. H), 3.45 (d, $J$ = 15.9, PhC*H*), 3.44 (s, O*Me*), 3.35 (d, $J$ = 15.9, PhC*H*). $^{13}$C-NMR (75 MHz, $CDCl_3$): 191.83, 171.31, 144.27, 137.86, 134.08, 133.34, 132.63, 130.64, 126.92, 51.77, 38.78. MS (CI): $m/z$ 272.1 (100, $[M + NH_4]^+$).

### 2-(*N*-9-Fluorenylmethyloxycarbonyl)aminomethyl-2′-carboxymethyl-biphenyl (15)

To $NH_2OH{\cdot}HCl$ (0.12 g, 1.47 mmol) and NaOMe (0.079 g, 1.47 m mol) in $H_2O$–MeOH (6 mL, 1 : 4), was added **9** (0.25 g, 0.98 mmol), heated at 50–55 °C for 16 h. The solvent was then removed and the residue partitioned between 1 N $NaHSO_4$ and EtOAc. The organic layer was dried ($MgSO_4$) and evaporated. Flash chromatography (silica, cyclohexane–EtOAc, 85 : 15) afforded the desired oxime as a pale yellow oil (0.2 g, 80%). $R_f$ (silica, cyclohexane–EtOAc 3 : 1) 0.24. $^1$H-NMR (300 MHz, $CDCl_3$): 7.89–7.08 (*m*, 10H, 8 arom. H, *H*C=N, OH), 3.47 (s, O*Me*), 3.42 (d, $J$ = 16.0, PhC*H*), 3.31 (d, $J$ = 16.0, PhC*H*). MS (CI): $m/z$ 270.1 (100, $[M + H]^+$). The oxime (0.26 g, 0.96 mmol) and 10% palladium on charcoal (0.06 g, 10% by wt) in methanol (5 mL), was stirred under hydrogen gas. Upon completion, the catalyst was removed by filtration through celite and washed with MeOH. Saturated aq. $Na_2CO_3$ was added and extracted with $CH_2Cl_2$. The organic layers were combined, dried over $Na_2SO_4$, and the solvent evaporated to afford the amine (**12**) $R_f$ (silica, EtOAc–MeOH 3 : 1): 0.18. The amine in EtOH (15 mL) and $H_2O$ (30 mL) was treated with NaOH (10 mL 10 N), refluxed for 16 h, to 25 °C, acidified to pH 2, and extracted with EtOAc. The combined organic layers were dried ($Na_2SO_4$) and concentrated to yield the amino acid. A suspension of the amino acid (1.9 g, 7.8 mmol) in dioxane (20 mL) was treated with 10% $Na_2CO_3$ (55 mL), cooled to 0 °C, treated with a solution of Fmoc-*O*-succinimide (Fmoc*O*Su) (2.4 g, 7.3 mmol) in dioxane (20 mL) over 15 min and stirred at rt for 1 h. Water (pH 3) was added, and extracted with EtOAc. The organic layer was dried and concentrated. Flash chromatography (silica, cyclohexane–EtOAc–AcOH 80 : 20 : 1) afforded the desired protected amino acid **15** (1.2 g, 56%). $R_f$ (silica, cyclohexane–EtOAc–AcOH 60 : 40 : 1): 0.2. Mp: 80–82 °C. IR ($CCl_4$): 3449 m, 3068 s, 1716 s. $^1$H-NMR (300 MHz, $CDCl_3$): 7.95–7.28 (m, 16 arom. H), 5.31 (br. s, N*H*), 4.53 (d, $J$ = 6.5, OC$H_2$), 4.30 (m, 3H, PhC*H*, PhC$H_2$), 3.68 (d, $J$ = 15.9, PhC*H*), 3.56 (d, $J$ = 15.9, PhC*H*). $^{13}$C-NMR (75 MHz, $CDCl_3$): 172.54, 156.10, 143.74, 133.16, 132.40, 119.94, 65.19, 46.67, 41.38, 38.42. MS (ESI): $m/z$ 486.1 (100, $[M + Na]^+$). HR-MS (CI): $m/z$ 464.1864 ($[M + H]^+$; $C_{30}H_{26}NO_4^+$, calc. 464.1856).

### 3-Methyl carboxymethyl-2′-formyl-biphenyl (10)

Was prepared by the same method as for **9** (see above) as a yellow oil. $R_f$ (silica, cyclohexane–EtOAc 3 : 1): 0.38. IR ($CHCl_3$): 1736 s, 1690 s. $^1$H-NMR (300 MHz, $CDCl_3$): 10.22 (s, CHO), 8.27–7.51 (m, 8 arom. H), 3.95 (s, O*Me*), 3.93 (s, 2H, PhC$H_2$). $^{13}$C-NMR (75 MHz, $CDCl_3$): 192.20, 171.53, 145.46, 137.96, 134.21, 133.66, 133.42, 127.49, 52.02, 40.88. MS (CI): $m/z$ 272.1 (100, $[M + NH_4]^+$).

### 3-(*N*-9-Fluorenylmethyloxycarbonyl)aminomethyl-2′-carboxymethyl-biphenyl (16)

Was prepared by the same method as for **15** (see above). $R_f$ (silica, cyclohexane–EtOAc–AcOH 60 : 40 : 1): 0.22. Mp: 145–146 °C. IR (KBr): 3409 m, 1813 m, 1790 m, 1739 s, 1713 s. $^1$H-NMR (300 MHz, DMSO): 7.68–7.13 (m, 16 arom. H), 4.88 (br. s, N*H*), 4.29 (d, $J$ = 6.8, OC$H_2$), 4.23 (d, $J$ = 5.7, PhC$H_2$), 4.09 (t,

$J$ = 6.7, PhC$H$), 3.59 (s, PhC$H_2$). $^{13}$C-NMR (75 MHz, $CDCl_3$): 172.51, 156.20, 143.74, 135.06, 130.04, 119.95, 65.20, 46.68, 41.41, 40.60. MS (ESI): $m/z$ 486.1 (100, [M + Na]$^+$). HR-MS (CI): $m/z$ 464.1870 ([M + H]$^+$; $C_{30}H_{26}NO_4^+$, calc. 464.1856).

### 3-Methyl carboxymethyl-3′-formyl-biphenyl (11)

Was prepared by the same method as for **9** (see above) as a yellow oil. $R_f$ (silica, cyclohexane–EtOAc 3 : 1): 0.42. IR (neat): 1732 s, 1694 s, 1600 m. $^1$H-NMR (300 MHz, $CDCl_3$): 10.19 (s, CHO), 8.21–7.37 (m, 8 arom. H), 3.824 (s, O$Me$), 3.819 (s, C$H_2$). $^{13}$C-NMR (75 MHz, $CDCl_3$): 192.12, 171.70, 141.75, 139.97, 136.84, 134.69, 132.98, 125.87, 52.00, 41.04. MS (CI): $m/z$ 272.2 (100, [M + $NH_4$]$^+$).

### 3-(*N*-9-Fluorenylmethyloxycarbonyl)aminomethyl-3′-carboxymethyl-biphenyl (17)

Was prepared by the same method as for **15** (see above). $R_f$ (silica, cyclohexane–EtOAc–AcOH 60 : 40 : 1): 0.19. Mp: 187–189 °. IR (KBr): 3345 m, 1734 m, 1698 s. $^1$H-NMR (300 MHz, DMSO): 7.69–7.19 (m, 16 arom. H), 5.58 (br. s, NH), 4.39 (s, 2H, $OCH_2$), 4.37 (s, 2H, PhC$H_2$), 4.17 (t, $J$ = 6.9, PhC$H$), 3.59 (s, 2H, PhC$H_2$). $^{13}$C-NMR (75 MHz, $CDCl_3$): 172.51, 156.22, 143.72, 135.66, 128.75, 119.93, 65.26, 46.63, 43.72, 40.67. MS (ESI): $m/z$ 486.1 (100, [M + Na]). HR-MS (CI): $m/z$ 464.1867 ([M + H]$^+$; $C_{30}H_{26}NO_4^+$, calc. 464.1856).

**Table 4**

| Peptide | $t_R$/min | MS ($m/z$) [M + H]$^+$ |
|---|---|---|
| **18** | 18.2, 18.5 | 1906.8 |
| **19** | 14.6 | 1906.7 |
| **20** | 14.5 | 1906.7 |
| **21a** | 13.2 | 748.9 |
| **21b** | 13.6 | 749.0 |

### Synthesis of peptidomimetics 18, 19, 20 and 21

The synthesis of mimetic **18** is a typical procedure: Fmoc-Arg(Pbf)-OH (1.2 equiv.) was coupled to 2-chlorotrityl chloride resin (1.08 mmol g$^{-1}$) in the presence of diisopropylethylamine (4 equiv.) in $CH_2Cl_2$. Following removal of the Fmoc group with 20% piperidine in *N*-methylpyrrolidine (NMP), chain elongation was performed sequentially with Fmoc-Lys(Boc)-OH (2×), Fmoc-Leu-OH, Fmoc-Arg(Pbf)-OH, Fmoc-Leu-OH, **15**, Fmoc-Val-OH, Fmoc-Arg(Pbf)-OH, Fmoc-Tyr($^t$Bu)-OH, Fmoc-Lys(Boc)-OH, Fmoc-Trp(Boc)-OH, and Fmoc-Arg(Pbf)-OH (each 4 equiv.), using 20% piperidine–NMP for Fmoc deprotection, HOBt–HBTU for activation, diisopropylethylamine as a base and NMP as solvent. After completion of the synthesis, the linear peptide was cleaved from the resin with 0.6% $CF_3COOH$ in $CH_2Cl_2$, and then cyclized overnight at RT in 1% diisopropylethylamine–dimethylformamide with HOBt and HBTU (3 equiv.). Deprotection with $CF_3COOH$–$iPr_3SiH$–$H_2O$ (95 : 2.5 : 2.5), precipitation with diethyl ether, followed by purification by preparative HPLC-MS ($C_{18}$ column, gradient 20–50% MeCN in $H_2O$ in 5 column volumes) gave **18** in 10% overall yield, and >95% purity by HPLC.

The retention times ($t_R$) on analytical $C_{18}$ reverse phase HPLC (Vydac C18 218TP104, 10 μm, 125 Å, 4 × 100 mm, 1 ml min$^{-1}$) using a gradient 5–50% MeCN in $H_2O$ (+0.1% TFA) in 3 column volumes, and the mass by ESI-MS are reported below:

### Antimicrobial assays

Innocula of each microorganism were diluted into Mueller–Hinton (MH) broth to give approximately $10^6$ colony forming units (CFU) per mL. Aliquots (50 μL) of the innocula were added to MH broth (50 μL) containing the peptide in serial twofold dilutions. Antimicrobial activities are expressed as the minimal inhibitory concentration (MIC) in μg mL$^{-1}$ at which 100% inhibition of growth was observed after 18–20 h incubation at 37 °C.

**Table 5** The $^1$H NMR assignments of peptides **21a** and **21b** are given below ($H_2O$–$D_2O$ 9 : 1, pH 3, 300 K):

| Residue | $^3J$(NHCαH) | NH | H-C(α) | H-C(β) | Others |
|---|---|---|---|---|---|
| **21a** | | | | | |
| Leu$^1$ | 5.2 | 7.72 | 3.67 | 1.42, 1.42 | CH(γ) 1.42; $CH_3$(δ) 0.86, 0.86 |
| Arg$^2$ | 5.6 | 8.55 | 3.96 | 1.86, 1.86 | $CH_2$(γ) 1.58, 1.58; $CH_2$(δ) 3.19, 3.19; NH(ε) 7.20 |
| Arg$^3$ | 7.7 | 8.15 | 4.17 | 1.78, 1.93 | $CH_2$(γ) 1.54, 1.54; $CH_2$(δ) 3.18, 3.18; NH(ε) 7.19 |
| Val$^4$ | 8.7 | 7.60 | 4.02 | 2.01 | $CH_3$(γ) 0.77, 0.87 |
| Biaryl$^5$ | — | 8.23 | | | (NH)$CH_2$ 4.15, 4.37 |
| | | | | | Phenyl ring (N-term.): H(δ$^1$) 7.35, H(ε$^1$) 7.45, H(ζ) 7.40, H(ε$^2$) 7.22 |
| | | | | | Phenyl ring (C-term.): H(δ$^1$) 7.41, H(ε$^1$) 7.22, H(ζ) 7.44, H(ε$^2$) 7.28 |
| | | | | | $CH_2$ (CO) 3.64, 3.76 |
| **21b** | | | | | |
| Leu$^1$ | 5.1 | 7.67 | 4.16 | 1.47, 1.47 | CH(γ) 1.55; $CH_3$(δ) 0.87, 0.91 |
| Arg$^2$ | 5.6 | 8.35 | 4.03 | 1.77, 1.85 | $CH_2$(γ) 1.56, 1.60; $CH_2$(δ) 3.18, 3.18; NH(ε) 7.20 |
| Arg$^3$ | 6.3 | 8.17 | 4.01 | 1.74, 1.89 | $CH_2$(γ) 1.50, 1.50; $CH_2$(δ) 3.14, 3.14; NH(ε) 7.16 |
| Val$^4$ | 8.0 | 7.84 | 3.91 | 2.16 | $CH_3$(γ) 0.91, 0.97 |
| Biaryl$^5$ | — | 8.16 | | | (NH)$CH_2$ 3.88, 4.57 |
| | | | | | Phenyl ring (N-term.): H(δ$^1$) 7.43, H(ε$^1$) 7.22, H(ζ) 7.42, H(ε$^2$) 7.22 |
| | | | | | Phenyl ring (C-term.): H(δ$^1$) 7.46, H(ε$^1$) 7.44, H(ζ) 7.40, H(ε$^2$) 7.23 |
| | | | | | $CH_2$ (CO) 3.52, 3.60 |

 

### Hemolytic activity

Fresh human red blood cells were washed three times with phosphate buffered saline (PBS), and then incubated with peptide at a concentration of 100 μg $mL^{-1}$ for 1 h at 37 °C. The final erythrocyte concentration was *ca.* $0.9 \times 10^9$ per mL. The values of 0% and 100% lysis were determined by incubation of cells with PBS or 0.1% Triton X-100 in water, respectively. The samples were centrifuged, the supernatant diluted 20-fold in PBS, and the optical density was measured at 540 nm.

## Abbreviations

Boc, *t*-butoxycarbonyl; DIEA, *N*,*N*′-diisopropylethylamine; DMF, *N,N*-dimethylformamide; Fmoc, [(9*H*-fluorenyl)-methoxy]carbonyl; HBTU, 2-[1*H*-benzotriazole-1-yl]-1,1,3,3-tetramethyluronium hexafluorophosphate; HOBt, *N*-hydroxy-benzotriazole; NCCLS, National Committee for Clinical Laboratory Standards (now, Clinical and Laboratory Standards Institute, CLSI); Pbf, 2,2,4,6,7-pentamethyldihydrobenzofuran-5-sulfonyl; NMP, *N*-methylpyrrolidone; TFA, trifluoroacetic acid.

## Acknowledgements

The authors thank the Swiss National Science Foundation for financial support.

## References

1 K. A. Brogden, *Nat. Rev. Microbiol.*, 2005, **3**, 238.
2 J. B. McPhee and R. E. W. Hancock, *J. Pept. Sci.*, 2005, **11**, 677.
3 M. Zasloff, *Nature*, 2002, **415**, 389.
4 D. Hopwood, S. Levy, R. P. Wenzel, N. Georgopapadakou, R. H. Baltz, S. Bhavnani and E. Cox, *Nat. Rev. Drug Discovery*, 2007, **6**, 8.
5 V. N. Kokryakov, S. S. L. Harwig, E. A. Panyutich, A. A. Shevchenko, G. M. Aleshina, O. V. Shamova, H. A. Korneva and R. I. Lehrer, *FEBS Lett.*, 1993, **327**, 231.
6 C. Q. Zhao, T. Ganz and R. I. Lehrer, *FEBS Lett.*, 1995, **368**, 197.
7 A. Aumelas, M. Mangoni, C. Roumestand, L. Chiche, E. Despaux, G. Grassy, B. Calas and A. Chavanieu, *Eur. J. Biochem.*, 1996, **237**, 575.
8 R. L. Fahrner, T. Dieckmann, S. S. L. Harwig, R. I. Lehrer, D. Eisenberg and J. Feigon, *Chem. Biol.*, 1996, **3**, 543.
9 C. Roumestand, V. Louis, A. Aumelas, G. Grassy, B. Calas and A. Chavanieu, *FEBS Lett.*, 1998, **421**, 263.
10 J. J. Buffy, A. J. Waring and M. Hong, *J. Am. Chem. Soc.*, 2005, **127**, 4477.
11 J. Chen, T. J. Falla, H. Liu, M. A. Hurst, C. A. Fujii, D. A. Mosca, J. R. Embree, D. J. Loury, P. A. Radel, C. C. Chang, L. Gu and J. C. Fiddes, *Biopolymers*, 2000, **55**, 88.
12 S. S. L. Harwig, A. Waring, H. J. Tang, Y. Cho, L. Tan and R. I. Lehrer, *Eur. J. Biochem.*, 1996, **240**, 352.
13 W. G. Jing, E. J. Prenner, H. J. Vogel, A. J. Waring, R. I. Lehrer and K. Lohner, *J. Pept. Sci.*, 2005, **11**, 735.
14 R. Mani, J. J. Buffy, A. J. Waring, R. I. Lehrer and M. Hong, *Biochemistry*, 2004, **43**, 13839.
15 R. Mani, A. J. Waring, R. I. Lehrer and M. Hong, *Biochim. Biophys. Acta: Biomembranes*, 2005, **1716**, 11.
16 J. A. Robinson, S. C. Shankaramma, P. Jetter, U. Kienzl, R. A. Schwenderner, J. W. Vrijbloed and D. Obrecht, *Bioorg. Med. Chem.*, 2005, **13**, 2055.
17 S. C. Shankaramma, Z. Athanassiou, O. Zerbe, K. Moehle, C. Mouton, F. Bernardini, J. W. Vrijbloed, D. Obrecht and J. A. Robinson, *ChemBioChem*, 2002, **3**, 1126.
18 S. C. Shankaramma, K. Moehle, S. James, J. W. Vrijbloed, D. Obrecht and J. A. Robinson, *Chem. Commun.*, 2003, 1842.
19 C. M. Nair, M. Vijayan, Y. V. Venkatachalapathi and P. Balaram, *J. Chem. Soc., Chem. Commun.*, 1979, 1183.
20 J. Späth, F. Stuart, L. Jiang and J. A. Robinson, *Helv. Chim. Acta*, 1998, **81**, 1726.
21 J. A. Robinson, *Synlett*, 2000, 429.
22 M. Kaiser, M. Groll, C. Siciliano, I. AssfalgMachleidt, E. Weyher, J. Kohno, A. G. Milbradt, C. Renner, R. Huber and L. Moroder, *ChemBioChem*, 2004, **5**, 1256.
23 R. Kannan and D. H. Williams, *J. Org. Chem.*, 1987, **52**, 5435.
24 V. Brandmeier and M. Feigel, *Tetrahedron*, 1989, **45**, 1365.
25 D. J. Suich, S. A. Mousa, G. Singh, G. Liapakis, T. Reisine and W. F. DeGrado, *Bioorg. Med. Chem.*, 2000, **8**, 2229.
26 R. B. Hopkins and A. D. Hamilton, *J. Chem. Soc., Chem. Commun.*, 1987, 171.
27 J. P. Schneider and J. W. Kelly, *Chem. Rev.*, 1995, **95**, 2169.
28 R. P. Cheng, D. J. Suich, H. Cheng, H. Roder and W. F. DeGrado, *J. Am. Chem. Soc.*, 2001, **123**, 12710.
29 P. Guntert, C. Mumenthaler and K. Wüthrich, *J. Mol. Biol.*, 1997, **273**, 283.
30 G. Müller, G. Hessler and H. Y. Decornez, *Angew. Chem., Int. Ed.*, 2000, **39**, 894.
31 E. Bunnenberg, C. Djerassi, K. Mislow and A. Moscowitz, *J. Am. Chem. Soc.*, 1962, **84**, 2823.
32 K. Mislow, E. Bunnenberg, R. Records, K. Wellman and C. Djerassi, *J. Am. Chem. Soc.*, 1963, **85**, 1342.
33 K. Mislow, M. A. W. Glass, R. E. O'Brien, P. Rutkin, D. H. Steinberg, J. Weiss and C. Djerassi, *J. Am. Chem. Soc.*, 1962, **84**, 1455.
34 R. W. Woody, *Adv. Biophys. Chem.*, 1992, **2**, 37.
35 *Methods for dilution antimicrobial susceptibility tests for bacteria that grow aerobically*, National Committee for Clinical Laboratory Standards, Wayne, PA, USA, 2007, approved standard 7th edn, M07-A7.